Received: 30 March 2023 | Revised: 8 July 2023 | Accepted: 9 July 2023

DOI: 10.1002/app.54469

RESEARCH ARTICLE

Journal of Applied Polymer Science WILEY

Evaluation of spherulite growth in PHB-based systems – A DoE approach

Katarzyna Majerczak | **John Liggat**

Department of Pure and Applied Chemistry, University of Strathclyde, Glasgow, UK

Correspondence
John Liggat, Department of Pure and Applied Chemistry, University of Strathclyde, 295 Cathedral Street, Glasgow G1 1XL, UK.
Email: j.j.liggat@strath.ac.uk

Funding information
Innovate UK Smart Sustainable Plastic Packaging, Grant/Award Number: NE/V010603/1

Abstract

Formulations based on poly(hydroxybutyrate) (PHB) and poly(hydroxybutyrate-*co*-valerate) were studied to statistically assess the importance of process parameters (temperature) and chemistry in filled and/or plasticized PHB-based formulations on spherulite growth rate (SGR) and nucleation density (ND). It was found that in binary systems, addition of a plasticizer results in shift of the maximum SGR towards lower temperatures, with the value of the shift dependent on polymer-plasticizer compatibility. The presence of the filler does not significantly influence SGR, instead resulting in ND changes dependent on filler chemistry, with Cloisite Ca^{++} showing the strongest nucleating action in all formulations among fillers studied. In ternary systems, statistical analysis shows that SGR strongly depends on the crystallization temperature (T_c), plasticizer type and concentration, and hydroxyvalerate content in the polymer chain while being independent of the presence and chemistry of the filler in the system. ND has, however, proven to be dependent on all investigated parameters, including both filler type and its concentration, with T_c being the most important factor. These results expand the understanding of factors controlling crystallization in polymer systems and provide an initial set of design tools that can be used to control mechanical properties in new generations of packaging materials.

KEYWORDS

boron nitride, Cloisite, copolymer, design of experiments, plasticizer, polarised light microscopy, Poly(hydroxybutyrate), spherulite growth

1 | INTRODUCTION

Plastic (including microplastic) pollution is one of the most challenging and prominent problems in modern world. The influence of plastic on many ecosystems, including aquatic, atmospheric, and terrestrial systems[1] is considered practically irreversible,[2] highlighting the need to reduce production and consumption of virgin plastics, improve the waste management systems,[2,3] as well as introduce more eco-friendly solutions to the market. One of the main contributors to the plastic pollution is plastic packaging, including plastic films.[4] These are often not recyclable due to infrastructure limitations, generating a need for their replacement with more eco-friendly alternatives.[5]

Among these, polyhydroxyalkanoates (PHAs) are promising candidates as, unlike petroleum-derived plastics, they are bacteria-synthesized, giving the possibility of structure (hence property) modification.[6,7] Further, PHAs

are biodegradable and biocompatible,[8] with mechanical properties similar to commonly used thermoplastics, good barrier properties, and compatibility with current manufacturing processes due to their melt-processability.[9] The most broadly studied member of PHA family is poly(hydroxybutyrate) (PHB) and its copolymer – poly (hydroxybutyrate-*co*-valerate) (PHBV).[10–12] PHB remains expensive to produce and has a narrow processing window – disadvantages that can be mitigated by changing the system chemistry and improving understanding of the links between processing conditions and the overall properties of the material.

Both PHB and PHBV exhibit a semicrystalline multiscale structure.[13] On the nano-scale, PHBV creates lamellae – crystalline regions embedded in the non-organized amorphous region. Lamellae stack, creating larger structures called microfibrils, which in turn organize radially, creating even larger structures with adjacent microfibrils – spherulites. Both degree of crystallinity and spherulitic microstructure (dependent on nucleation density, ND, and spherulite growth rate, SGR) control solid state properties of the plastic materials, including mechanical properties.[14,15] Specifically, changing spherulite size leads to changes in degree of crystallinity (increasing with increasing spherulite size)[16] and crack propagation (running either circumferentially around the spherulites or radially through them).[17] The control over both ND and SGR (hence crystallinity and microstructure) can be therefore used to optimize the properties of the final product.

Pure PHB materials crystallize readily, leading to the creation of highly crystalline, brittle materials.[18] Among the ways of tuning crystallization in the system are changing HV content,[19,20] controlling crystallization conditions (e.g., crystallization temperature, T_c),[21] as well as introducing additives to the system.[22] The most popular additives are plasticizers (that reduce the brittleness of the matrix) and nucleating fillers (that influence overall number of created crystals due to acting as a heterogeneous nucleation centre). As we have shown in our review,[23] while many studies have investigated the effect of additives on the crystallization behavior of PHB at given conditions, it is currently challenging to provide an unambiguous trend in the system behavior upon introducing different additives to the system due to variations in processing methods and additive properties. Moreover, the vast majority of research focuses on the influence of single additive at fixed processing conditions. Therefore, there is no systematic way of assessing the effect of each parameter (e.g., changes in system chemistry or processing conditions) on the resulting system properties in complex formulations that mimic real-life products.

Design of experiments (DoE) is a method that uses analysis of variance (ANOVA) to plan and analyze experiments as well as interpret them to obtain information about the effects of each individual variable on the results, identify interactions between the variables, and model the outcome using a mathematical function. DoE enables making conclusions about simultaneous changes of multiple parameters, preventing often inconclusive results obtained from experiments where parameters are changed one at a time.[24] Specifically, full-factorial design (FFD) provides information about all of the potential interactions within a system, while other systematic designs such as response surface design (RSD) are better suited to account for non-linear relationships between control parameters and their outcomes. Results obtained from DoE allow the exclusion of statistically insignificant terms to minimize the number of parameters in the system, in turn reducing processing costs and enabling control of the final product.

This work aims to improve the understanding of the crystallization behavior in PHB-based systems and assess the importance of processing conditions (T_c) and composition – HV content, plasticizer chemistry and plasticizer concentration ($X_{plasticizer}$), filler chemistry and filler concentration (X_{filler}) – on the spherulitic crystallization (i.e., SGR, ND, nucleation time, kinetics of crystallization, and morphology of the spherulites) in multi-component formulations. This way, we will assess the statistical importance of each factor and interactions between the individual factors with a view to establishing formulation design criteria not only for PHB, but also other polymers that show similar crystallization behavior.

2 | MATERIALS AND METHODS

2.1 | Materials

Pure PHB and its copolymer, PHBV (HV content of 7, 12, and 21 mol%) with thermal properties as presented in Table 1, were obtained from Zeneca Bio Products and purified by Soxhlet extraction in ethanol followed by drying at 40°C prior to usage. HV content for all samples was confirmed via nuclear magnetic resonance

TABLE 1 Thermal properties of studied PHBV powders measured by differential scanning calorimetry. T_g stands for glass transition temperature, while T_{m1} and T_{m2} correspond to the first and second melting peak, respectively. Uncertainty values represent one standard deviation around the mean ($n = 5$).

	T_g/°C	T_{m1}/°C	T_{m2}/°C
PHB	4.0 ± 0.1	175.1 ± 0.5	—
7% HV	1.8 ± 0.3	167.6 ± 0.3	—
12% HV	10.9 ± 0.4	138.9 ± 0.3	159.3 ± 0.2
21% HV	−1.5 ± 0.2	116.5 ± 0.6	148.8 ± 0.6

TABLE 2 Factors and factor values used for full- and partial factorial design (FD).

Factor	Code	Factor values				FFD concerned
		1	2	3	4	
T_c/°C	A	70	90	110	—	FF1 & FF2
X_{filler}/wt %	B	0	1	5	—	FF1 & FF2
Filler type (–)	C	No filler	$CaCO_3$	CCa^{++}	CNa^{+}	FF1 & FF2
$X_{plasticizer}$/wt %	D	0	10	20	—	FF2
Plasticizer type	E	No plasticizer	TA	ATBC	—	FF2
HV content /mol%	F	0	7	12	21	FF1

measurements. Triacetin (TA, Sigma–Aldrich, W200700, 99%) and acetyl tributyl citrate (ATBC, Sigma–Aldrich, W308005, ≥98%) were used as plasticizers, while Cloisite Na^{+} and Ca^{++} (BYK, denoted as CNa^{+} and CCa^{++}, respectively, with available technical information presented elsewhere[25]) and calcium carbonate (Sigma–Aldrich, C4830, ≥99%) were used as fillers. Plasticizer and fillers were used as received.

2.2 | DoE analysis

Minitab 20 was used for matrix creation and data analysis. The experiments were divided into 6 separate sets regarding system chemistry: (1) Pure PHB samples; (2) Plasticized PHB samples; (3) Filled PHB samples; (4) Filled and plasticized PHB samples; (5) Pure PHBV samples; (6) Filled PHBV samples.

For the analysis, two separate groups were created: (1) to assess the effect of HV content, filler chemistry and concentration in unplasticized samples (sets 1, 3, 5, and 6) on SGR and ND; (2) to assess the effect of plasticizer chemistry and concentration as well as filler chemistry and concentration in pure PHB matrix (without effect of HV content, sets 1, 2, 3, and 4) on SGR and ND. They were denoted as full-factorial 1 (FF1, with 83 formulations and 4 factors studied) and full-factorial 2 (FF2, with 105 formulations and 5 factors studied), respectively. Experiments were performed in random order (i.e., not by sets) to avoid any potential biases.

Each composition was investigated at three T_cs. The temperature range chosen for investigations was based around the T_c of the maximum SGR for pure PHB ($T_{c\ max}$) used in this study (90°C, vide infra) and minimum T_c at which SGR could be reliably detected (70°C, vide infra). Concentrations of the fillers and plasticizers were based on the limits commonly used in literature and industry and were chosen as 1 and 5 wt% for fillers and 10 and 20 wt% for plasticizers, with respect to the polymer concentration. Plasticizers used in this study were already proven to be compatible with PHB.[26–28]

Full-factorial design (FFD) was utilized to create a matrix of formulations to be investigated to assess which parameters affect SGR and ND in the PHB-based systems. This design was chosen as FFD has been proven to create better models compared to the other methods.[29] Further, alternative design choices such as central composite design were not appropriate for use in this study due to their incompatibility with categorical variables (i.e., plasticizer and filler types) and requirement for non-physical formulations (i.e., negative values of additive content). The main drawback of FFD – using only first-order equations (linear regression) – was overcome by supplementing with RSD which implements quadratic terms in the response equation to account for possible non-linear correlations in the system.

All datasets met the assumptions required for ANOVA (the residuals are independent, normally distributed, and with approximately equal variance; all input factors are independent of one another). The complete set of parameters and factor values used for each FFD is summarized in Table 2.

2.3 | Film preparation

Plasticized polymer powder was prepared by mixing polymer and plasticizer in desired mass ratio. As-prepared powders were left overnight to allow diffusion of the plasticizer into the polymer to improve its distribution. Filler was incorporated by mixing with either plasticized or unplasticized polymer in the desired mass ratio. Ca. 3 mg of mixed powder was placed between two round ethanol-cleaned cover slips and melted on the hot plate at 200°C for 1 min, followed by sample analysis on the hot stage of the polarized microscope pre-set at the desired T_c.

2.4 | Polarized microscopy

Measurements were performed using Dino-lite Edge AM73915MZTL polarized microscope coupled with the

additional polarizer (Dino-Lite BL-ZW1) and the hot stage (Linkam TMS 94). The spherulitic growth behavior was recorded in a movie format that was further transformed into snapshots. Radial spherulitic growth rate and ND (presented as number of spherulites (NS) in the observation window of 2 mm diameter) was determined by analyzing the snapshots at a given time using ImageJ software. All samples but pure PHB were analyzed at three T_cs: 70, 90 and 110°C, while pure PHB samples were crystallized within the temperature range 30–140°C, with increments of 10°C to assess changes in SGR with T_c as the initial step. 2 h measurement time was considered a practical limit for tracking nucleation as most of the samples fully crystallized within 15 min. If spherulites were observed within 2 h, the measurement was continued until spherulites covered the observation window fully.

3 | RESULTS AND DISCUSSION

In section 3.1, we first discuss the changes in spherulite crystallization (i.e., SGR, ND, and spherulite morphology) for pure PHB systems as a benchmark, followed by assessing the effect of changes in system chemistry by one parameter at the time (i.e., addition of plasticizer and/or filler as well as changes in polymer backbone by introducing HV groups) on these parameters. Then, investigations into more complex systems (i.e., filler and plasticizer addition or filler addition and changes in HV content) as a mimic of real-world formulations are presented. Finally, in section 3.2. a statistical evaluation of multiple factors using DoE analysis is implemented to deconvolute the importance of each factor.

3.1 | Spherulitic crystallization in PHB-based systems

3.1.1 | Effect of T_c in pure PHB systems

Pure PHB samples studied here can be characterized by a normal-like distribution of SGR with changes in T_c (Figure 1a), with maximum SGR recorded at 90°C. Below 70°C, reliable detection of the spherulite growth rate was not possible due to very high ND (Figure 2a) and consequent short time (<2 s) of growth for an individual spherulite. Based on these results, three temperatures were chosen for further experiments on all other investigated formulations: 90°C (corresponding to the maximum SGR), 70°C (minimum temperature ensuring reliable spherulite detection), and 110°C (to ensure the same temperature step between the temperature of maximum SGR and other investigated temperatures).

High ND at low T_c results in creation of voids (likely air) that are pushed to the front of growing spherulites due to fast rearrangement of polymer chains. At high T_c (>120°C), however, the ND is low (Figure 1b) and nucleation times are prolonged (>1 h compared to <10 s and < 40 s at 70 and 90°C, respectively). In general, the shorter the nucleation time, the higher ND in the system (Figure 2a–c). Moreover, recorded SGR decreased more than two orders of magnitude while increasing the T_c from 90 to 140°C (0.19 mm/min vs. 0.0013 mm/min recorded at 90 and 140°C, respectively, Figure 1a).

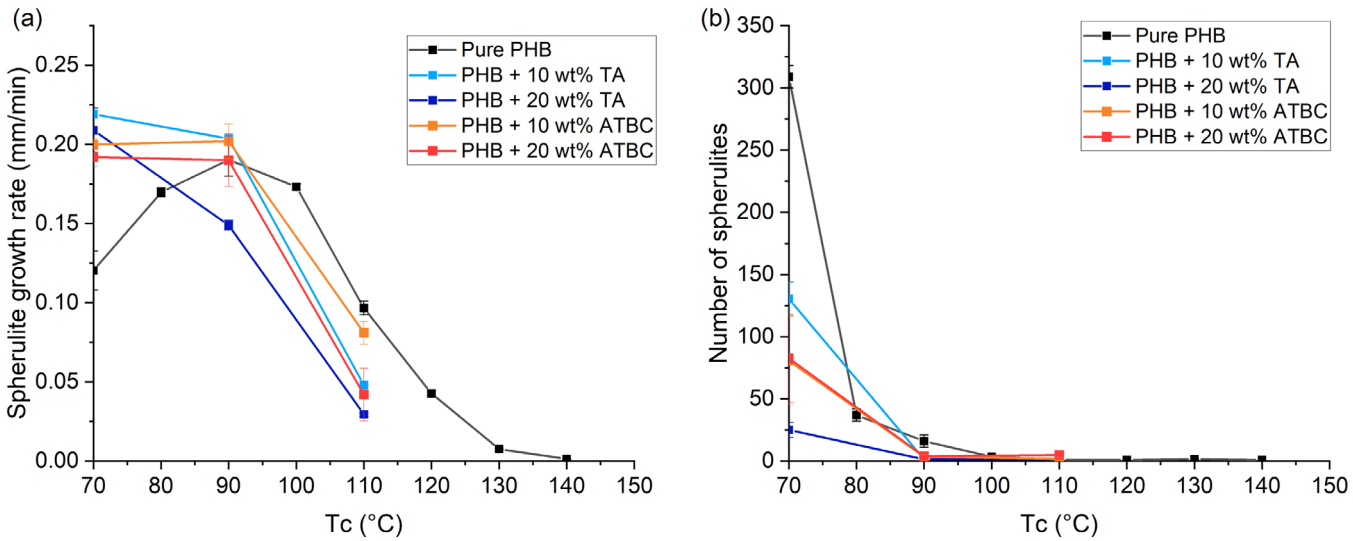

FIGURE 1 Dependence of (a) SGR and (b) NS on T_c for pure and plasticized PHB samples. [Color figure can be viewed at wileyonlinelibrary.com]

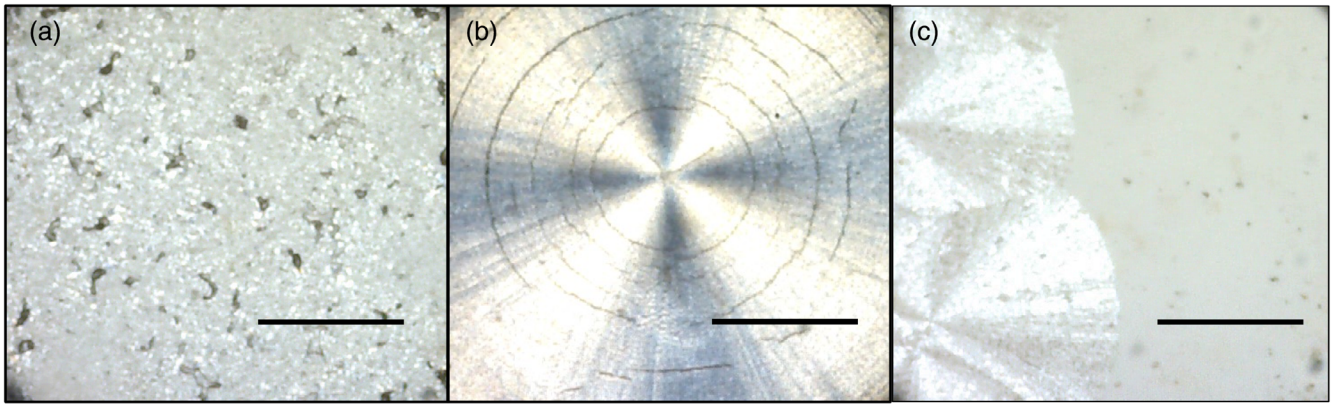

FIGURE 2 Polarized microscopy image of PHB crystallized at (a) 30°C, (b) 110°C and (c) 130°C after t = 2 h. The scale bar corresponds to 500 μm. [Color figure can be viewed at wileyonlinelibrary.com]

Recorded $T_{c\ max}$ and overall SGR values are in line with values reported previously.[30–32] For pure PHB, experimental error at $T_{c\ max}$ is higher than for other investigated temperatures. $T_{c\ max}$ corresponds to the maximum growth rate and, consequently, the temperature of maximum heat release rate. This has the potential to cause localized fluctuations in temperature at the growth front and is particularly important as the maximum crystallization rate is a point of balance between the enhanced driving force for crystallization and polymer mobility reduction.[33] Consequently, any fluctuations in temperature can lead to SGR fluctuations and the observed higher experimental error bars.

According to Hoffman, there are three distinct regimes of polymer crystal growth that describe the competition between the nucleation rate and diffusive displacement rate:[34–37] (1) regime I – at low supercooling, where rate of spreading is significantly greater than rate of nucleation, resulting in large size of individual spherulites, (2) regime II – at medium supercooling, where several spherulites nucleate and grow, with the separation between individual spherulites decreasing with decreasing T_c, and (3) regime III – at high supercooling, where no spreading takes place and the separation between the individual spherulites is of the same order as molecular width, resulting in high number of spherulites of small size. These different regimes give rise to various spherulite morphologies, with non-banded spherulites observed in regimes I and III, and banded spherulites observed in regime II.[35] Here, the banded spherulite structure was observed at T_cs in the range 70–120°C, with increasing band spacing with increasing T_c due to greater diffusion length of melt molecules, in line with literature reports.[34,35]

While there is still discussion about the growth mechanism for banded spherulites, models based on the stress-induced lamellar twisting[38–43] and rhythmic crystal growth with consequent depletion zone[38,40,44] are widely accepted. Other models have been proposed,[45–47] however, all models state lamellar packing and growth as the main reason for band structure of the spherulites. Indeed, in PHB systems band spacing was previously related to periodical change of the lamellar orientation and spherulite thickness fluctuation, indicating the origin of the banded spherulites in agreement with lamellar twist and rhythmic crystal growth models.[34] Further, the depletion zone at the growth front is a result of slow diffusion rate as a limiting step of the spherulite growth and volume shrinkage during crystallization solidification process.[35]

At 130°C, the intermediate morphology between non-banded and banded spherulites is observed (Figure 2c), with concentrated rings of increased waviness of the front line. From 140°C, however, non-banded spherulite morphology was observed due to faster diffusion and lack of depletion zone in the crystal growth front.

3.1.2 | Effect of T_c and plasticizer in PHB systems

Plasticizers increase flexibility of individual polymer chains by reducing polymer-polymer interactions and consequently increasing system free volume,[30,48] hence influencing their molecular motion and crystallizing ability. The choice of the plasticizer depends on the polymer-plasticizer compatibility, thermal stability, as well as toxicity. Plasticizers used in this study are non-toxic and can be used in bio-friendly packaging materials.

Upon introducing plasticizer to the PHB system, the maximum of the SGR versus T_c function shifts to lower T_cs – the higher the plasticizer concentration, the more significant the shift (Figure 1a). This shift is alike that of lowering glass transition T_g (4.0°C for pure PHB compared to −10.4 and − 19.7°C for 10 and 20 wt% of TA, respectively, or −6.9 and −17.7°C for 10 and 20 wt% of

ATBC, respectively) and melting temperature T_m (175.1°C for pure PHB compared to 169.5 and 164.4°C for 10 and 20 wt% of TA, respectively, or 172.4 and 168.7°C for 10 and 20 wt% of ATBC, respectively) upon the addition of the plasticizer. Observed behavior is a consequence of increased mobility and freedom of movement of individual polymer chains hence lower energy required for either crankshaft motion or melting of polymer crystals. A similar phenomenon of maximum SGR shifts towards lower temperatures with plasticizer addition was previously reported for PHB and polylactic acid plasticized with triethyl citrate[30] and triphenyl phosphate,[49] respectively. However, no dilution effects due to the plasticizer presence are observed here as SGR values are not decreasing upon plasticizer addition (Figure 1a).

The effect of plasticizer addition is therefore similar to that of thermal energy. At low temperatures, the free volume in the system and translational energy are lower compared to higher temperatures, resulting in increased probability of chain entanglement and stable nucleus creation. Accordingly, nucleation rate is faster than crystallization rate leading to creation of a larger number of small spherulites. Conversely, at higher temperatures individual polymer chains have higher energy reducing the rate of stable nucleus formation and increasing the nucleation time – hence creating a lower number of spherulites of significantly increased size.

When both factors increasing the polymer translational energy and free volume are present (i.e., elevated temperature and presence of plasticizer), their effect is combined, resulting in a shift of the maximum SGR to lower temperatures which can be tuned by the chemistry of the plasticizer. Here, TA has more significant effect on PHB-based systems than ATBC. While ATBC has higher molar mass than TA (resulting in lower number of molecules in the polymer matrix for the same mass concentration), the shift for 20 wt% ATBC introduced to the system is less significant than that of 10 wt% TA, suggesting that TA is more compatible with PHB-based systems than ATBC.

This hypothesis can be further supported by the nucleation times recorded for each system (Table 3). While there is no difference in their values recorded for pure PHB films and formulations plasticized with 10 wt% ATBC at T_c equal to 70 or 90°C, introducing 10 wt% TA to the system is sufficient to cause significant delay at $T_c = 90$°C (nucleation time equal to ca. 2 min cf. <10 s). For both plasticizers used, nucleation time increases to 5 min at $T_c = 110$°C at 10 wt% additive concentration (compared to 30 s for pure PHB). Increasing concentration of TA up to 20 wt% leads to slightly longer nucleation times – however, the trend of shorter nucleation time recorded for ATBC remains consistent. Regardless of the plasticizer chemistry, lower ND was noted in plasticized systems due to lower supercooling compared to pure PHB,[30] with ND decreasing with increasing plasticizer concentration (Figure 1b). However, in general higher ND was reported for ATBC addition compared to samples plasticized with TA.

Compatibility in discussed systems can also be assessed based on Hansen solubility parameter-based distance between two molecules (R_a):

$$R_a^2 = 4(\delta_{D1} - \delta_{D2})^2 + (\delta_{P1} - \delta_{P2})^2 + (\delta_{H1} - \delta_{H2})^2 \quad (1)$$

where δ_D, δ_P and δ_H are dispersion, polar, and hydrogen bonding components, respectively, contributing to the total cohesive energy of the system (summarized in Table 4 for polymer and plasticizers used in this study). The smaller R_a, the higher likelihood that the two molecules will be compatible. In discussed systems, R_a is equal to 4.95 and 6.97 for PHB-TA and PHB-ATBC, respectively, indicating that TA is more compatible plasticizer. This is in line with both our nucleation time results and previously reported observations, where tributyl citrate (structurally similar to ATBC molecule) showed poor incorporation into PHB matrix and did not influence the Young's modulus of the system.[50] Therefore, the distribution of ATBC in PHB matrix is likely to be less uniform than that of TA.

In terms of spherulitic growth kinetics, the change of spherulite radius with time is typically linear, with the SGR calculated as the gradient of this function[54] (Figure 3, blue). Upon introducing plasticizer to the system, however, some positions were characterized by non-linear behavior, with SGR dependent on the time (Figure 3,

TABLE 3 Nucleation times for pure and plasticized PHB systems as a function of temperature.

$X_{plasticizer}$		$T_c = 70$°C	$T_c = 90$°C	$T_c = 110$°C
N/A	0 wt%	<10 s	<10 s	30 s
TA	10 wt%	<10 s	Ca. 2 min	Ca. 5 min
	20 wt%	20 s	Ca. 2 min	Ca. 6 min
ATBC	10 wt%	<10 s	<10 s	Ca. 5 min
	20 wt%	10 s	20 s	Ca. 5 min

TABLE 4 Hansen solubility parameters for polymers and plasticizers used in this study.

	δ_D	δ_P	δ_H
PHB[51]	15.5	9.0	8.6
TA[52]	16.5	4.5	9.1
ATBC[53]	16.9	2.7	7.6

black) – the longer crystallization time, the slower SGR as the tangent of the function decreases over time. This behavior is more prominent in samples with higher plasticizer concentration and was observed in samples plasticized with both TA and ATBC.

Plasticizer in polymer systems hinder chain packing and crystallization as a result of increased free volume in the system. Further, additives with low molecular weight present in the polymer matrix lead to inclusion defects and hence influence the perfection of individual crystallites.[55,56] The majority of the additives are present in the amorphous region of the polymer – both within interlamellar regions of microfibrils or in the regions outside the spherulite front.[57] It was previously shown that mechanical properties of the polymers are changed due to the slow crystallization as a result of additive rejection from a spherulite.[58] We suggest that the non-linear behavior observed here is a result of plasticizer migration during spherulite creation and its accumulation at the spherulite front, leading to decreased SGR as either longer time for spherulite growth is needed in well-plasticized environment or increased concentration of plasticizer in the amorphous region within the spherulite leads to increased diffusion time outside the spherulite. This behavior is not, however, universally observed in plasticized PHB systems and was not recorded for triethyl citrate up to 30 wt% plasticizer addition.[55] For consistency, the SGR for plasticized systems was calculated in the same way as for other samples (gradient of the linear regression fit), with R^2 values equal to ca. 0.98, indicating very good fit despite described deviations from linear behavior.

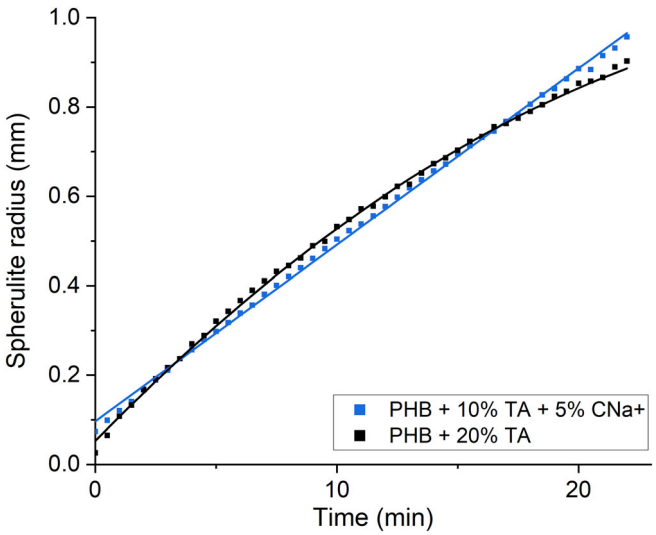

FIGURE 3 Spherulite radius growth with time for plasticized PHB samples with/without the addition of a filler at 110°C. [Color figure can be viewed at wileyonlinelibrary.com]

In terms of spherulitic morphology, no significant changes were noted compared to pure PHB samples (Figure 4). A characteristic Maltese cross was observed for all formulations, with maximum spherulite size growing to >1 mm at 110°C. In some formulations with ATBC slightly asymmetrical spherulite growth was observed (Figure 4c), however, the deviation from ideal spherulite was not significant. Moreover, after introducing a plasticizer to PHB matrix, regardless of its chemistry, the band spherulite structure is still observed at T_c s in the range 70–110°C, however, becomes less prominent compared to pure PHB structure observed at the same T_c. It is therefore suggested that while plasticizer influences the perfection of the individual lamellae and changes packing within spherulites, the shift in $T_{c\ max}$ does not happen in parallel with changes in morphology.

3.1.3 | Effect of T_c and filler in PHB systems

Addition of the filler up to 5 wt% does not result in significant change in SGR, independent of the filler concentration or chemistry (Figure 5a). In general, presence of the filler creates a physical obstruction for polymer

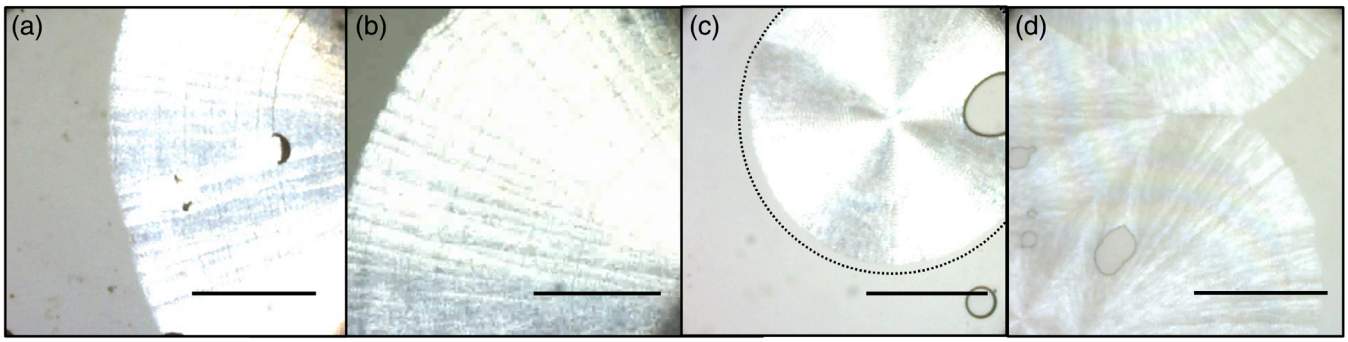

FIGURE 4 Polarized light microscope images of PHB film with the addition of (a) 10 wt% TA, (b) 20 wt% TA, (c) 10 wt% ATBC, and (d) 20 wt% ATBC. All images were collected at Tc = 110 °C. The scale bar corresponds to 500 μm, while the dashed circle represents size of the spherulite assuming perfect spherical shape. [Color figure can be viewed at wileyonlinelibrary.com]

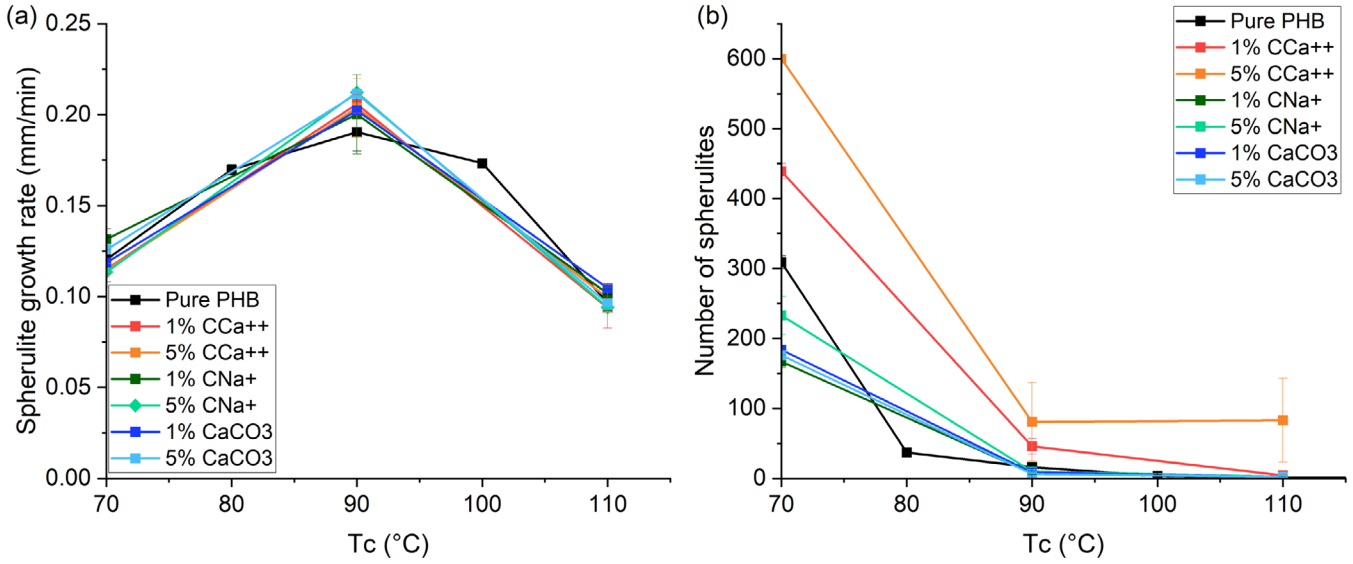

FIGURE 5 Effect of filler in PHB system on (a) SGR and (b) NS as a function of T_c. [Color figure can be viewed at wileyonlinelibrary.com]

chains to move. Further, when the favorable polymer-filler interactions are present, there is a need to introduce additional energy to break these interactions and induce lamella formation.[59] Hence, both of the mentioned factors influence polymer chain mobility and the rate of primary crystallization. Here, this reduction was not observed for SGR, suggesting little to no effect of mentioned parameters.

For modified clays, reduction of crystallization rate calculated using differential scanning calorimetry was previously observed, with simultaneous change of the crystallization mechanism from regime II to regime III.[60] This indicates increase in nucleation rate in the system, which was also observed in formulations herein. This effect was dependent on the chemistry of the filler, with CCa^{++} showing the most prominent increase in the NS in the system (Figure 5b). $CaCO_3$ and CNa^+ slightly increased the ND in the system only at $T_c = 110°C$ compared to pure PHB formulations – the ND (the number of spherulites per 4π mm^2 area) were recorded at 1 for pure PHB; 5 and 83 for 1 and 5 wt% addition of CCa^{++} at 90°C, respectively, compared to 2 and 3 for both CNa^+ and $CaCO_3$ at respective concentrations.

For PHBV systems, it has previously been shown that the addition of $CaCO_3$ resulted in slight drop in ND that was related to surface treatments of the filler,[61] while CNa^+ dispersed poorly in PHB films due to its high hydrophilicity.[62] The variation in nucleating action between fillers studied here might therefore arise due to the differences in the intermolecular interactions (despite both cloisites having a cationic nature), their aggregation behavior, and the existence of crystallographic relationships between the filler and polymer crystalline structure.[63]

On the macroscale, no changes in overall spherulitic morphology were observed upon introduction of the filler in the system independent of its concentration (Figure 6), with banded morphology noted for all formulations in the 70–110°C temperature range.

3.1.4 | Effect of T_c and HV content in PHB systems

Copolymers of PHB with various HV content are widely known to increase the processability window compared to pure PHB (reduction of T_m as reported in Table 1) and reduce its brittleness because of changes in the crystallizing properties of the matrix.[64,65] Increasing HV content leads to decreased SGR compared to pure PHB systems (Figure 7a). Introducing bulkier side groups to the polymer chain influences its flexibility by creation of additional steric obstructions that affect polymer chain folding and packing and prevents stable nucleus formation initiating polycrystalline aggregation and spherulite growth.[57] This behavior of decreasing SGR with increasing HV content is like that of poly(3-hydroxybutyrate) (P(3HB)) with increasing concentration of 4-hydroxybutyrate (4HB) groups.[66] However, no significant shift in $T_{c\ max}$ with changes in HV content was observed here.

Together with increasing SGR, the nucleation times increase with increasing HV content in PHB matrix – recorded at 30 s, 1 min, and 2.5 min for pure PHB, 7% HV and 12% HV, respectively – with no nucleation observed at 110°C for over 2 h for 21% HV sample (hence no SGR recorded, Figure 7a). HV content also influences NS in the system – the higher HV content, the lower NS

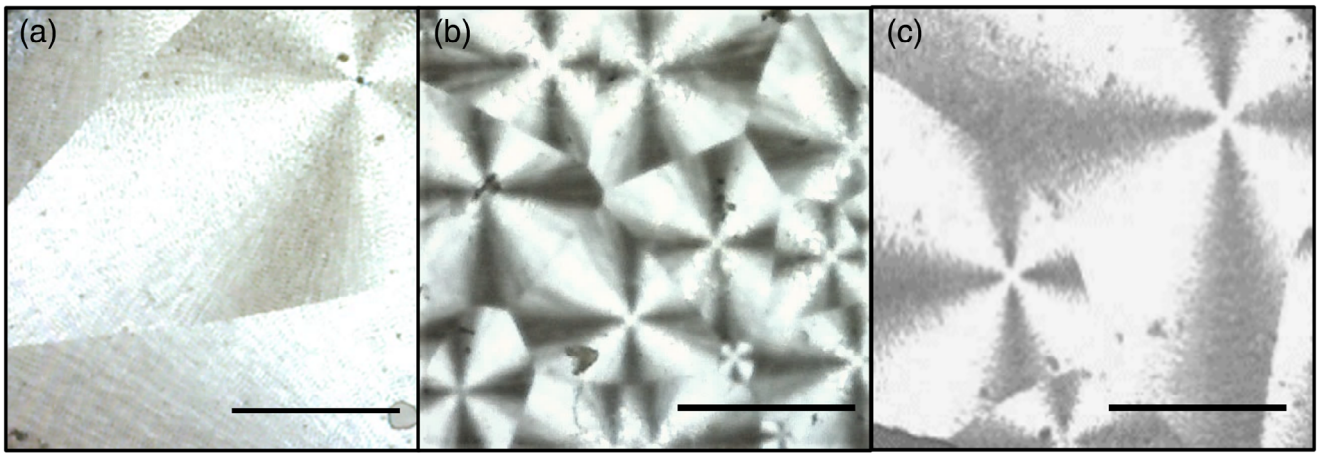

FIGURE 6 Polarized microscopy images of spherulites obtained at $T_c = 110°C$ in (a) PHB with 1 wt% CCa^{++}, (b) PHB with 5 wt% CCa^{++}, (c) PHB with 5 wt% CNa^{+}. The scale bar corresponds to 500 μm. [Color figure can be viewed at wileyonlinelibrary.com]

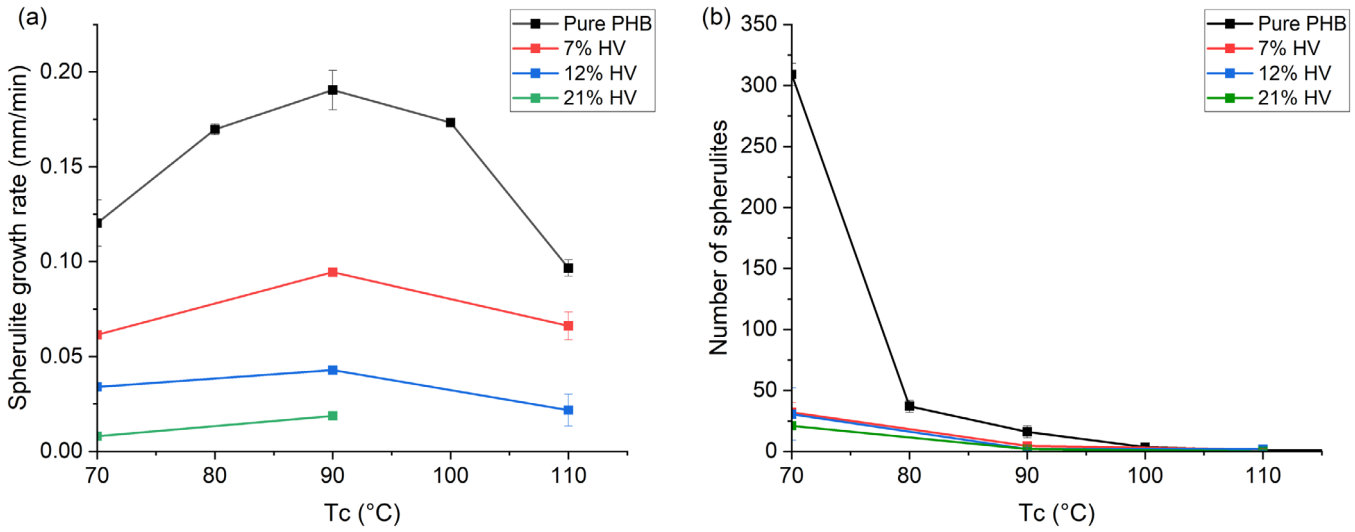

FIGURE 7 Effect of HV content on (a) SGR and (b) NS as a function of T_c. [Color figure can be viewed at wileyonlinelibrary.com]

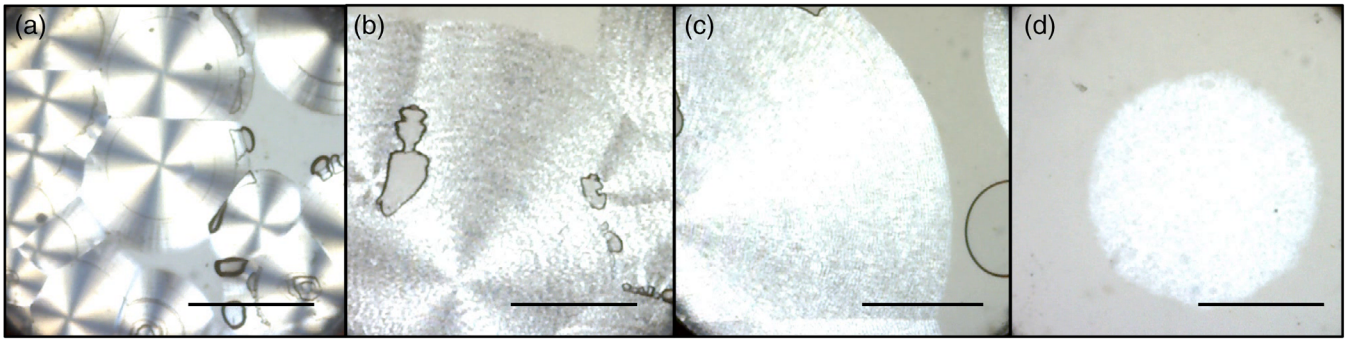

FIGURE 8 Polarized microscope images at $T_c = 90°C$ of (a) pure PHB, (b) 7% HV, (c) 12% HV, and (d) 21% HV. The scale bar corresponds to 500 μm. [Color figure can be viewed at wileyonlinelibrary.com]

(Figure 7b), highlighting the importance of steric obstruction effects in PHB-based systems.

In terms of the spherulitic morphology, the Maltese cross became less prominent with increasing HV content until disappearing at 21% HV (Figure 8). For this sample, no banded spherulite structure is observed at either 70 or 90°C, with change of the morphology similar to the shift from category I to category II[67,68] observed with

increasing T_c. For other investigated HV contents, however, banded spherulite structure was observed. Moreover, similar to pure PHB samples (Figure 2c), crack-like concentric rings,[69] different to optical band structure, are created. These rings are created further away from spherulite nucleation centre and were previously identified as characteristic for PHBV formulations. Their origin was related to density differences between crystalline part of the spherulite and supercooled melt, respective decrease in volume and creation of negative pressure that forces supercooled melt to flow into the vacuum caused by volume decrease in PHBV matrix.[69] While this phenomenon is unlikely for films of <50 μm thickness,[69] this explanation is plausible for films investigated here.

3.1.5 | Effect of T_c, filler and/or plasticizer in PHBV systems

Upon introducing both additives to the pure PHB system (i.e., filler and plasticizer, FF2 design), the kinetics of spherulitic growth rate was linear, deviating from trends observed for unfilled plasticized PHB systems (Figure 3, blue) – however, non-symmetrical spherulites with more irregular outer edges were created for both investigated chemistries of the plasticizer (Figure 9). In these samples, SGR was dependent on the growth direction. This resulted in SGR variation up to 100% as the SGR in the direction of the fastest growth was twice as high as the one measured in the direction of slowest growth (e.g., 0.0269 mm/min and 0.0549 mm/min for PHB sample filled with 5 wt% CCa^{++} and plasticized with 20 wt% ATBC and T_c at 110°C). When comparing the maximum SGR for filled and plasticized formulations against plasticized formulations without filler, the average SGRs in the former case were not significantly different to the latter (Figure S1 in the Supporting Information). We speculate that observed asymmetrical growth of the spherulites might be a result of non-uniform distribution of the filler that creates a physical obstruction for polymer chain to fold and prevents plasticizer migration to the spherulite front. Hence, the spherulite growth directions at which

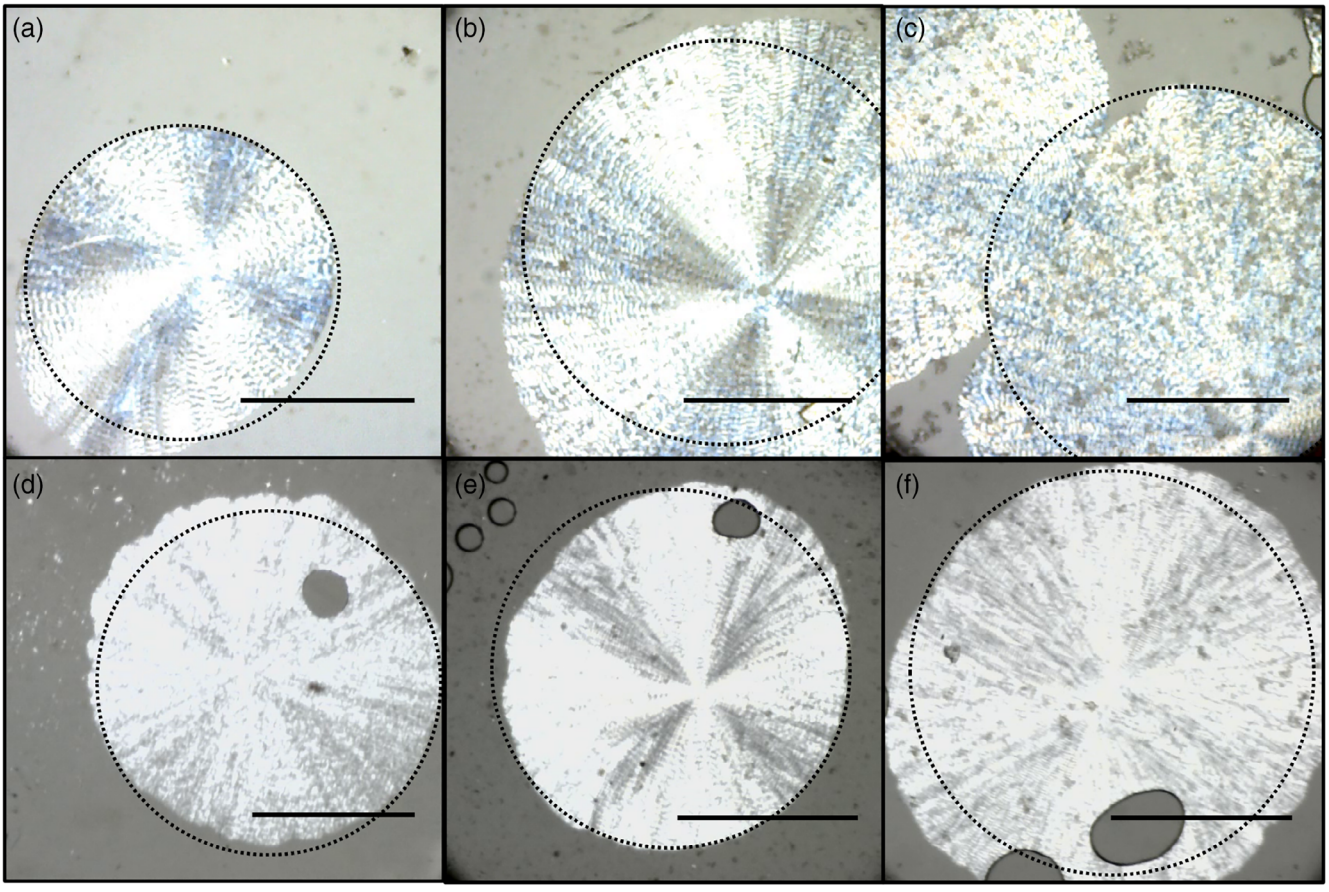

FIGURE 9 Polarized microscope images at $T_c = 110°C$ of PHB plasticized with: 20 wt% TA and addition of (a) 5 wt% CNa^+, (b) 5 wt% CCa^{++}, (c) 5 wt% $CaCO_3$; 20 wt.% ATBC and addition of (d) 5 wt% CNa^+, (e) 5 wt% CCa^{++}, (f) 1 wt% $CaCO_3$. The scale bar corresponds to 500 μm, while the dashed circle represents size of the spherulite assuming perfect spherical shape. [Color figure can be viewed at wileyonlinelibrary.com]

high SGR was recorded is likely to have lower local concentration of the filler than directions with low SGR. Despite the variation in morphology, Maltese cross is still observed, with banded spherulite structure noted for all investigated formulations (Figure 9).

While considering unplasticized filled PHBV systems (FF1 design), introducing filler to 7% HV and 12% HV matrices resulted in the trend of SGR dependence on T_c similar to that of PHB except formulations with 5 wt% CCa^{++} that caused decrease in average SGR across T_c studied (Figure S2 in the Supporting Information). For 21% HV formulations, addition of the filler, independent of its chemistry, resulted in significant deviations in SGR with respect to T_c (Figure S2) that can be caused by either steric effects as a result of filler presence or errors in analysis caused by poorly-defined spherulite edges for these formulations (Figure 8d).

In terms of ND in plasticized samples (FF2 design), fillers and plasticizers had opposing effects to one another – fillers increased ND due to the increase in heterogeneous nucleation sites, while plasticizers decreased ND due to increased chain mobility. CCa^{++} had a greater effect on ND than CNa^{+} and $CaCO_3$ at any concentration (Figure S1 in the Supporting Information). In unplasticized PHBV formulations (FF1 design), introducing the filler increased ND for all investigated chemistries (Figure S2 in the Supporting Information), while for pure PHB systems only incorporation of CCa^{++} led to a net increase of ND. Moreover, addition of any filler to 21% HV samples at 110°C led to reduced nucleation times of under 2 h, enabling analysis, in contrast to the unfilled counterpart.

As the chemical complexity of the formulations increases, so does the nature of interactions between chemical species present in the system.[16] In order to systematically identify the effect of each parameter on both SGR and ND, as well as to identify parameters which significantly interact with one another, factorial experimental design combined with ANOVA were implemented.

3.2 | Statistical analysis of spherulitic crystallization in PHB-based systems

FFD and RSD were implemented to investigate the effect of each parameter on SGR and ND both in unplasticized (i.e., filled systems with various HV content, Table 2, FF1) and plasticized (i.e., filled PHB systems of various plasticizer content, two types of plasticizer studied, Table 2, FF2) formulations. FFD was used as the primary screening tool to investigate the complex interactions between the considered factors. Despite the model having four (FF1) or five (FF2) parameters, only interactions up to third order were considered for this initial analysis as higher-level interactions are often too complex to produce unambiguous results. Third-order interactions are unlikely to be important in real-life settings,[70] however, they can provide useful insight into the interplay between components in the systems studied here and were therefore not omitted. These results were further expanded by RSD to account for non-linear character of the SGR changes with T_c (Figure 1a).

3.2.1 | Spherulite growth rate in pure and filled PHBV systems (FF1 design)

For filled PHBV systems, linear regression of SGR against the system parameters was predicted with high accuracy ($R^2 = 0.99$, R^2 adjusted $= 0.98$), signifying a very good description of the system behavior without overfitting errors. To detect the importance of individual factors and their interactions on SGR, a Pareto plot was used that shows the magnitude of the standardized effects – from the largest to the smallest – as well as a reference line, the value of which is dependent on the defined α value[71] (here 0.05). Any factor that surpasses the reference line is likely to have a significant influence on the outcome. From the Pareto plot for FFD analysis in the unplasticized system (Figure 10a) one can conclude that only T_c and HV content as well as their interactions (included in the model as $x_1 \cdot x_2$ term) play important roles in the final SGR value. The presence of filler (neither concentration nor its chemistry) does not influence SGR in the ternary system, which is in line with results obtained from binary systems (Figure 5a).

As SGR dependence on T_c is not linear (Figure 1a), RSD was performed on the same set of data as FFD analysis, resulting in a fit of good accuracy ($R^2 = 0.90$, R^2 adjusted $= 0.88$). The variation in the R^2 values compared to FFD analysis is likely due to the lower number of terms considered during RSD analysis (which only considered binary interactions between parameters). The Pareto plot obtained from this analysis (Figure 10b) therefore extends the results obtained from FFD analysis – the second-order term of not only T_c but also HV content is statistically important for predicting SGR. Further, first order terms for these parameters as well as their interactions need to be included in the model to achieve satisfactory accuracy.

Interaction plots (Figure S3 in the Supporting Information) can be used to visually represent if the effect of one variable is dependent on another variable by comparing the differences in sensitivity from low to high levels (i.e., slope of obtained lines). In simple terms, they can be described as (i) no interactions for parallel lines, (ii) synergistic interactions for diverging lines, and (iii)

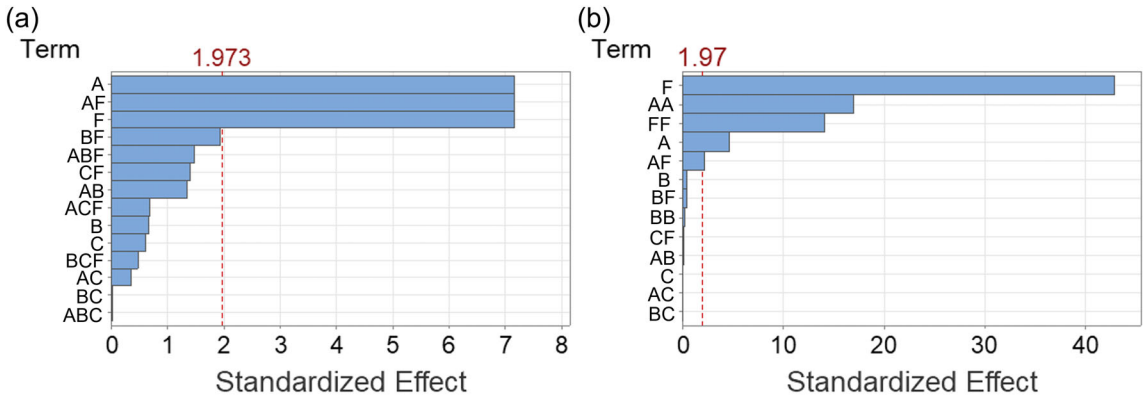

FIGURE 10 Pareto plot of the standardized effects with response as SGR for pure and filled PHBV formulations, $\alpha = 0.05$, obtained from: (a) FFD analysis, (b) RSD analysis. Symbols in the figure correspond to parameters as presented in Table 2. [Color figure can be viewed at wileyonlinelibrary.com]

antagonistic interactions for converging lines.[72] However, the interaction plots alone cannot be used to assess the statistical importance of the discussed interactions and need to be paired with ANOVA.

In systems studied here, visible interactions are noted for T_c and HV content (antagonistic interactions, Figure 7b), with little to no interactions between other pairs of parameters. For instance, any change in filler type and/or concentration causes at maximum a ca. 5% change in SGR, hence no effects visible in Figure S3. Regardless, weak interactions (no significant variation in the slope between different levels of parameters) are present for other pairs of parameters than T_c-HV content and as they are statistically not important (Figure 10a), they can be omitted in the final SGR formula.

Upon elimination of the statistically non-important factors from RSD analysis, the equation describing SGR in this system takes form presented as the contour plot (Figure 11). The complete set of equations from RSD analysis presenting SGR as a function of T_c, HV content, and X_{filler} for each filler type as a categorical value as well as after elimination of statistically unimportant parameters (backward elimination) is presented in the Supporting Information (Table S1 in the Supporting Information). We have shown that in the discussed system RSD analysis provides natural extension of the FFD analysis and can be used to establish statistically important factors influencing model outcome.

3.2.2 | Spherulite growth rate in filled, plasticized systems (FF2 design)

Modeling SGR in plasticized systems using FFD gives high accuracy ($R^2 = 0.97$, R^2 adjusted $= 0.96$). From this analysis, seven parameters that influence SGR were

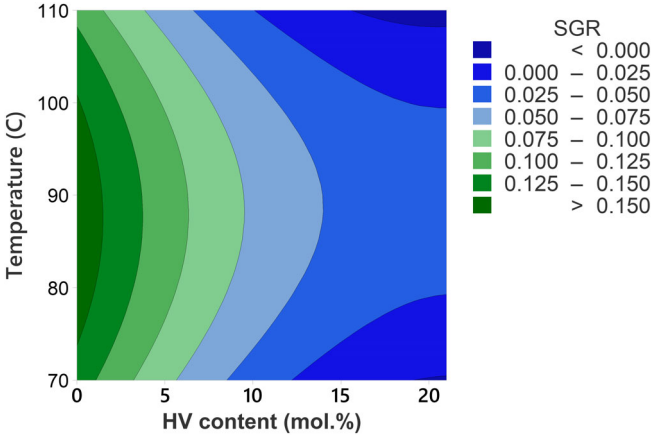

FIGURE 11 Contour plot of SGR as a function of T_c and HV content in filled PHBV formulations. [Color figure can be viewed at wileyonlinelibrary.com]

identified, namely T_c, plasticizer type and $X_{plasticizer}$, as well as second- and third-order interactions between these parameters (i.e., AE, AD, DE, and ADE, Figure 12a, Table 2). The influence of filler concentration and its chemistry on SGR remains insignificant, neither in the form of first order parameters nor as interactions with other statistically important factors, in line with results obtained for unplasticized ternary systems (Figure 10a).

While performing RSD analysis ($R^2 = 0.87$, R^2 adjusted $= 0.86$), T_c is the dominant factor as both first- and second-order terms have the highest standardized effect (Figure 12b). However, first-order terms of neither $X_{plasticizer}$ nor plasticizer type are important at 5% significance level. Instead, their interactions with T_c as well as the second-order term of $X_{plasticizer}$ are listed as parameters to be included in the model, indicating that either the shift of $T_{c\ max}$ with increasing plasticizer concentration (Figure 1d) is of non-linear character, or the

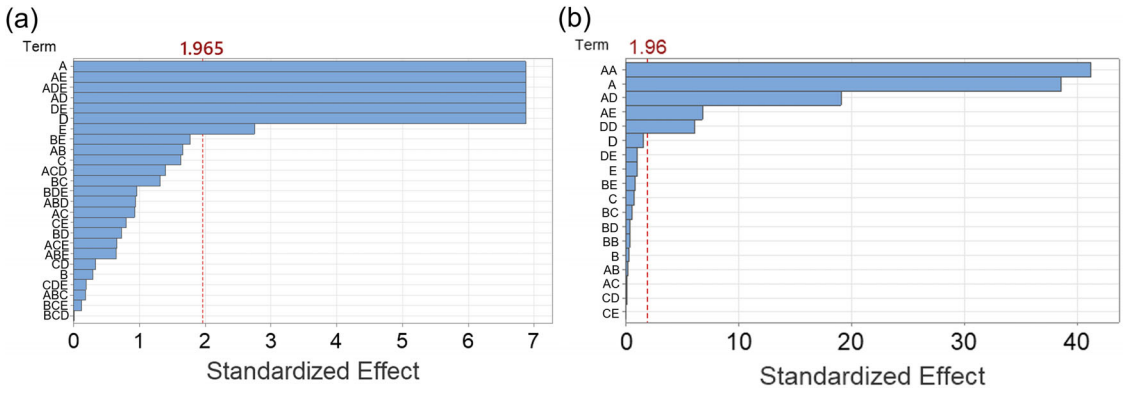

FIGURE 12 Pareto plot of the standardized effects with response as SGR for plasticized formulations, $\alpha = 0.05$, obtained from: (a) FFD analysis, (b) RSD analysis. Symbols in the figure correspond to parameters as presented in Table 2. [Color figure can be viewed at wileyonlinelibrary.com]

behavior between a plasticized and unplasticized system is discontinuous (i.e., the system behavior cannot be described using a single function). The second-order term of plasticizer type cannot be included in the model due to the categorical nature of this variable. The contour plot from RSD analysis for TA as a plasticizer of choice is presented in Figure 13, while the complete set of equations describing SGR as a function of Tc, X_{filler} and $X_{plasticizer}$ for each filler-plasticizer pair as well as SGR function after backward elimination is presented in the Supporting Information (Table S2 in the Supporting Information).

Overall, the nature of two-way interactions becomes more complex due to the presence of higher number of parameters. Similarly to unplasticized systems, few to no interactions are visible for any parameter (T_c, $X_{plasticizer}$ and plasticizer type) with X_{filler} or filler type, indicated by approximately parallel lines in respective graphs (Figure S4 in the Supporting Information). For interactions included in SGR model, their character changes within the T_c range investigated, indicating complex interactions that do not follow a clear trend. The considered T_c range can be therefore divided into separate regions (i.e., before and after $T_{c\ max}$) if a smaller T_c range is considered. For instance, while strong antagonistic interactions are present between TA and ATBC as a function of T_c in the 70–90°C range, they become synergistic in the 90–110°C range.

3.2.3 | Nucleation density in pure and filled PHBV systems (FF1 design)

FFD and RSD were also implemented to assess the influence of system chemistry and process parameters on ND, here represented as NS recorded in the observation window of the heated stage of diameter equal to 2 mm.

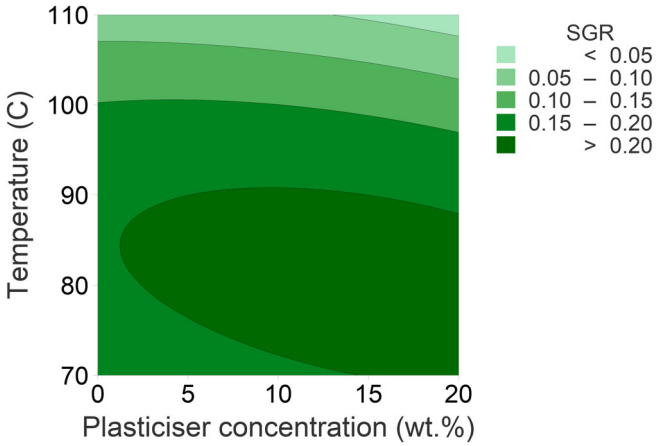

FIGURE 13 Contour plot of SGR as a function of T_c and HV content, with TA as a plasticizer of choice. [Color figure can be viewed at wileyonlinelibrary.com]

While it was possible to obtain satisfactory results from FFD analysis ($R^2 = 0.89$, R^2 adjusted = 0.82), decreased R^2 compared to SGR analysis suggests decreasing quality of the dependent variable fit using independent variables, while decreased R^2 adjusted show that some variables are not contributing to the model.

ND behavior in the discussed systems vary compared to the trends observed for SGR as both filler type and X_{filler} contribute to overall function, resulting in first-order terms for all parameters being statistically significant (i.e., T_c, HV content, X_{filler} and filler type, Figure 14a). Among fillers studied, CCa^{++} remained the most significant nucleating agent in ternary systems, with exemplary values of NS recorded at 129 and 600 for 1 and 5 wt% CCa^{++} in 7% HV formulations crystallized at 90°C compared to 6 and 8 spherulites and 5 and 7 spherulites observed for both filler concentrations for samples filled with CNa^{+} and $CaCO_3$, respectively. However, all fillers

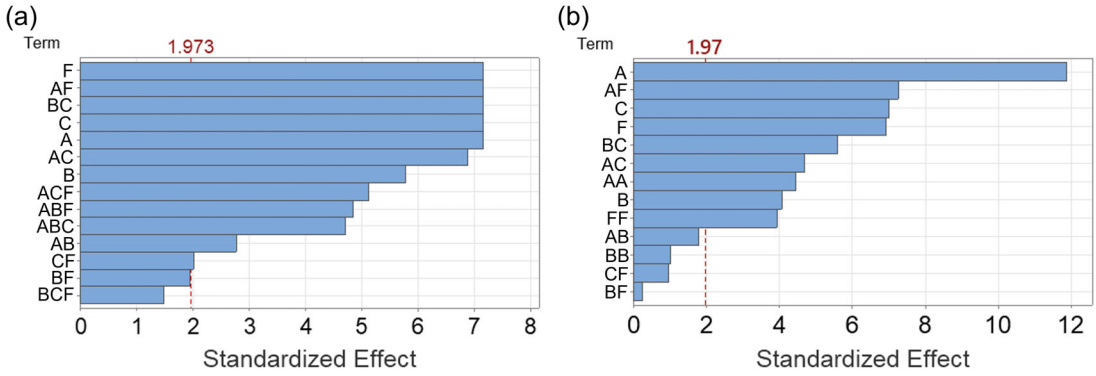

FIGURE 14 Pareto plot of the standardized effects with response as NS for unplasticized samples, $\alpha = 0.05$, obtained from: (a) FFD analysis, (b) RSD analysis. Symbols in the figure correspond to parameters as presented in Table 2. [Color figure can be viewed at wileyonlinelibrary.com]

show nucleating action in PHBV systems as spherulites in 21% HV sample at 110°C were observed – a phenomenon that was not recorded for samples without filler due to significant slowdown in nucleation rate upon increasing HV content in polymer backbone.

FFD analysis signifies the importance of interactions on the ND as all interactions but BF and BCF (Table 2) are to be included in the model at 5% significance level (Figure 14a). Considering statistically important two-way interactions, the character of AF interactions remains convoluted (Figure S5 in the Supporting Information). However, there is overall synergistic interaction between X_{filler} & T_c and X_{filler} & filler type, and an antagonistic interaction between HV content & filler type and T_c & filler type.

The RSD analysis results in lower quality fit ($R^2 = 0.63$, R^2 adjusted $= 0.60$), that is likely the consequence of fitting a second-order polynomial to the data that abruptly changes across investigated T_c range (i.e., changes in NS from 306 to 1 for crystallization in pure PHB at 70°C and 110°C, respectively), while minimizing the non-physical negative values for NS. Regardless, the conclusions from this analysis suggest that second order terms of both HV content and T_c are likely to be important factors in a predictive NS model (Figure 14b). Further, both X_{filler} and filler type are included in the quadratic equation, together with three pairs of two-way interactions (AF, BC, and AC, Table 2), in line with results obtained from FFD analysis. It is therefore concluded that while RSD analysis and resultant quadratic model are not the most accurate representation of the results in this instance, they provide valuable insight into the non-linear aspects of the effect of each parameter on ND in unplasticized systems. The contour plot from RSD analysis presented as a function of HV content and T_c with fixed values at 5 wt% CCa^{++} is presented in Figure 15, while the full set of equations for NS for each filler is presented in the Supporting Information (Table S3 in the Supporting Information).

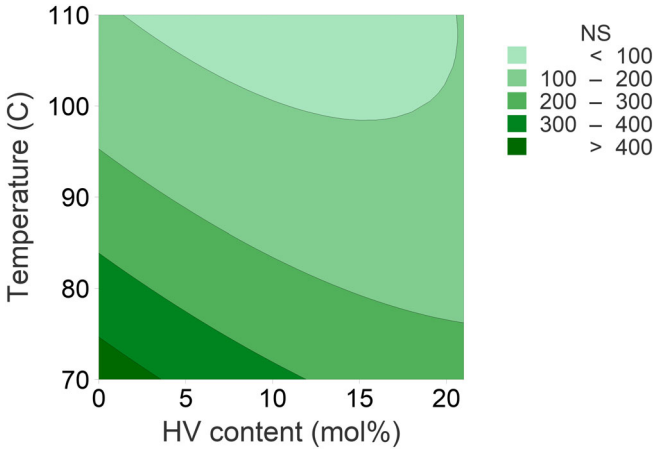

FIGURE 15 Contour plot of NS as a function of T_c and HV content, with fixed values at 5 wt% of the CCa^{++}. [Color figure can be viewed at wileyonlinelibrary.com]

3.2.4 | Nucleation density in filled plasticized PHB systems (FF2 design)

FFD analysis performed on ND in plasticized systems results in a high accuracy model ($R^2 = 0.95$, R^2 adjusted $= 0.94$), indicating all considered parameters (i.e., T_c, $X_{plasticizer}$, plasticizer chemistry, X_{filler}, and filler chemistry) influence the output at 5% significance level and should be included in the model as first-order terms (Figure 16a). Further, all pairs of two-way and three-way interactions aside from ABE and BE (Table 2) are of statistical significance, hence suggesting that ND in this system, similarly to unplasticized formulations, is influenced by all parameters with similar magnitude (standardized effect in Figure 16a).

Interestingly, the influence of individual parameters changes for RSD (Figure 16b). The model fit is improved compared to model of ND in unplasticized formulations

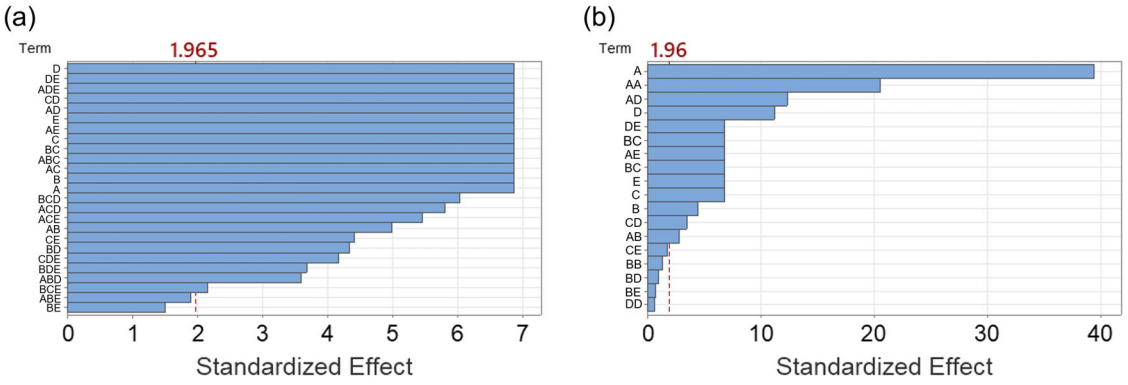

FIGURE 16 Pareto plot of the standardized effects with response as NS for plasticized samples, $\alpha = 0.05$, obtained from: (a) FFD analysis, (b) RSD analysis. Symbols in the figure correspond to parameters as presented in Table 2. [Color figure can be viewed at wileyonlinelibrary.com]

($R^2 = 0.83$, R^2 adjusted $= 0.83$). Here, the model indicated that T_c (both first- and second-order terms) is of the highest importance, which is an intuitive conclusion in line with observations described in Section 3.1. Further, first-order terms of all investigated factors are statistically important in the model (in line with FFD analysis), and their standardized effect decreases in order: $T_c > X_{plasticizer} >$ plasticizer type > filler chemistry > X_{filler}. Controlling the chemistry of the filler in plasticized systems therefore emerges as a more effective way of controlling ND than introducing higher amount of less effective filler. In plasticized systems, independent of the plasticizer type, CCa^{++} had the most profound effect on nucleation. Typical values of NS were recorded as 13 and 16 for 1 and 5 wt% CCa^{++} for formulations plasticized with 10 wt% TA crystallized at 90°C compared to 3 and 4 spherulites observed for both filler concentrations for samples filled with CNa^{+} and $CaCO_3$, respectively.

For RSD analysis, the number of two-way interactions that should be included in the model decreases compared to FFD model (i.e., CE, BD, and BE that should be excluded from quadratic model vs. BE that should be excluded from FFD model). Indeed, no interactions were noted for the X_{filler}-plasticiser type, while antagonistic interactions were observed for filler type-$X_{plasticizer}$ and $X_{plasticizer}-T_c$ pairs of parameters, and synergistic interactions were noted between plasticizer chemistry & $X_{plasticizer}$. For other pairs of parameters, either few to no interactions were noted or they showed non-linear dependence changing within the investigated constraints (Figure S6 in the Supporting Information).

ND in plasticized system shows more complex relationship between the independent variables and dependent variable (NS), with all factors contributing to the resultant ND at 5% significance level. While RSD analysis results in significantly lower R^2 compared to FFD analysis, it provides additional insight into system dynamics and allows to interpret the importance of each parameter in line with the results obtained for both binary systems. The resultant contour plot with fixed values at 5 wt% CCa^{++} and TA as a plasticizer type is shown in Figure 17, while the full set of equations for NS for each filler-plasticizer pair is presented in the Supporting Information (Table S4 in the Supporting Information).

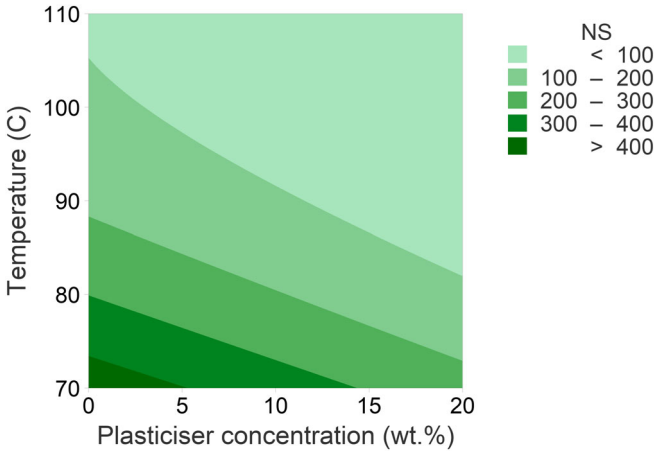

FIGURE 17 Contour plot of NS as a function of T_c and HV content, with fixed values at 5 wt% of the CCa^{++} and TA as a plasticizer type. [Color figure can be viewed at wileyonlinelibrary.com]

4 | CONCLUSIONS

In this study, factors influencing spherulitic crystallization in filled and plasticized PHBV systems were investigated using systematic experimental design and statistical analysis. We have found that in pure PHB systems, SGR is characterized by a normal distribution that does not change form upon varying the HV content in polymer chain, but with decreasing SGR recorded with increasing

HV content. Plasticizers and fillers have a different effect on spherulitic crystallization in the investigated systems. The presence of plasticizer results in the shift of $T_{c\ max}$ towards lower temperatures due to higher flexibility of the polymer chains. Conversely, the filler at concentrations up to 5 wt% does not have a significant influence on SGR in PHB system, resulting in similar SGR rate compared to pure PHB formulations. Further, while plasticizer addition leads to overall decrease in ND in polymer matrix, fillers show nucleating action, with nucleation efficiency dependent on the filler chemistry.

In ternary systems (filled PHBV or plasticized and filled PHB), SGR strongly depends on the T_c, HV content in the polymer chain (in unplasticized systems), as well as the amount of plasticizer introduced to the system and its chemistry (in plasticized systems). However, it remains independent of the presence of the filler in the system – both its concentration and chemistry. ND shows a significant dependence on all factors studied (i.e., T_c, HV content, plasticizer chemistry, $X_{plasticizer}$, filler chemistry, and X_{filler}) and can be controlled by chemistry and concentration of the additives at fixed crystallization conditions. We have shown that TA is more compatible plasticizer than ATBC, while CCa^{++} has the strongest nucleating action in all formulations. T_c was proven to be the most important parameter influencing both SGR and ND. The statistical analysis in the form of RSD models enabled consideration of non-linear character of variable change within the parameter limits studied and has shown that T_c, HV content and $X_{plasticizer}$ all show quadratic character of influence on SGR and ND.

AUTHOR CONTRIBUTIONS

Katarzyna Majerczak: Conceptualization (supporting); data curation (lead); formal analysis (lead); investigation (lead); methodology (equal); writing – original draft (lead). **John Liggat:** Conceptualization (lead); funding acquisition (lead); methodology (equal); project administration (lead); resources (equal); supervision (lead); validation (lead); writing – review and editing (lead).

ACKNOWLEDGMENTS

This research was funded by an Innovate UK Smart Sustainable Plastic Packaging grant (NE/V010603/1). The authors would like to thank Dr Karen Johnston for reviewing the draft manuscript. The authors would also like to thank Dr Karen Johnston, Dr Paul Mulheran, Dr Dominic Wadkin-Snaith and Dr Vitor Magueijo for helpful discussions regarding the presented results.

CONFLICT OF INTEREST STATEMENT

The authors declare no conflicts of interest.

DATA AVAILABILITY STATEMENT

Data underpinning this publication are openly available from the University of Strathclyde Knowledge Base at https://doi.org/10.15129/77d20d47-183e-41ff-bd9a-907bf73657f3.

ORCID

John Liggat https://orcid.org/0000-0003-4460-5178

REFERENCES

[1] P. Li, X. Wang, M. Su, X. Zou, L. Duan, H. Zhang, *Bull. Environ. Contam. Toxicol.* **2021**, *107*, 577.
[2] M. MacLeod, H. P. H. Arp, M. B. Tekman, A. Jahnke, *Science* **2021**, *373*, 61.
[3] W. W. Y. Lau, Y. Shiran, R. M. Bailey, E. Cook, M. R. Stuchtey, J. Koskella, C. A. Velis, L. Godfrey, J. Boucher, M. B. Murphy, R. C. Thompson, E. Jankowska, A. Castillo Castillo, T. D. Pilditch, B. Dixon, L. Koerselman, E. Kosior, E. Favoino, J. Gutberlet, S. Baulch, M. E. Atreya, D. Fischer, K. K. He, M. M. Petit, U. R. Sumaila, E. Neil, M. V. Bernhofen, K. Lawrence, J. E. Palardy, *Science* **2020**, *369*, 1455.
[4] T. D. Moshood, G. Nawanir, F. Mahmud, F. Mohamad, M. H. Ahmad, A. AbdulGhani, *Curr. Res. Green Sustain. Chem.* **2022**, *5*, 100273.
[5] R. Banerjee, S. S. Ray, *Macromol. Mater. Eng.* **2022**, *307*, 2100794.
[6] A. Steinbüchel, H. E. Valentin, *FEMS Microbiol. Lett.* **1995**, *128*, 219.
[7] B. Hazer, A. Steinbüchel, *Appl. Microbiol. Biotechnol.* **2007**, *74*, 1.
[8] P. Xing, L. Dong, Y. An, Z. Feng, M. Avella, E. Martuscelli, *Macromolecules* **1997**, *30*, 2726.
[9] M. Koller, A. Mukherjee, *Bioengineering* **2022**, *9*, 74.
[10] Z. Zheng, F.-F. Bei, H.-L. Tian, G.-Q. Chen, *Biomaterials* **2005**, *26*, 3537.
[11] Y. Deng, K. Zhao, X.-F. Zhang, P. Hu, G.-Q. Chen, *Biomaterials* **2002**, *23*, 4049.
[12] G. Eke, A. M. Kuzmina, A. V. Goreva, E. I. Shishatskaya, N. Hasirci, V. Hasirci, *J. Mater. Sci. Mater. Med.* **2014**, *25*, 1471.
[13] J. Yang, H. Zhu, Y. Zhao, Q. Jiang, H. Chen, G. Liu, P. Chen, D. Wang, *Eur. Polym. J.* **2017**, *91*, 81.
[14] H. W. Starkweather Jr., R. E. Brooks, *J. Appl. Polym. Sci.* **1959**, *1*, 236.
[15] J. H. Magill, *J. Mater. Sci.* **2001**, *36*, 3143.
[16] A. M. El-Hadi, *Polym. Bull.* **2014**, *71*, 1449.
[17] J. K. Hobbs, T. J. McMaster, M. J. Miles, P. J. Barham, *Polymer* **1996**, *37*, 3241.
[18] J. Li, M. F. Lai, J. J. Liu, *J. Appl. Polym. Sci.* **2004**, *92*, 2514.
[19] S. Modi, K. Koelling, Y. Vodovotz, *Eur. Polym. J.* **2011**, *47*, 179.
[20] T. L. Bluhm, G. K. Hamer, R. H. Marchessault, C. A. Fyfe, R. P. Veregin, *Macromolecules* **1986**, *19*, 2871.
[21] Z. škrbić, V. Divjaković, *Polymer* **1996**, *37*, 505.
[22] S.-G. Hong, T.-K. Gau, S.-C. Huang, *J. Therm. Anal. Calorim.* **2011**, *103*, 967.
[23] K. Majerczak, D. Wadkin-Snaith, V. Magueijo, P. Mulheran, J. Liggat, K. Johnston, *Polym. Int.* **2022**, *71*, 1398.
[24] B. Durakovic, *Period. Eng. Nat. Sci. (PEN)* **2017**, *5*, 5.
[25] H. Petersen, I. Jakubowicz, J. Enebro, N. Yarahmadi, *Appl. Clay Sci.* **2015**, *107*, 78.

[26] A. Chaos, A. Sangroniz, A. Gonzalez, M. Iriarte, J.-R. Sarasua, J. Del Río, A. Etxeberria, *Polym. Int.* **2019**, *68*, 125.
[27] J. Y. Cho, S. H. Kim, H. J. Jung, D. H. Cho, B. C. Kim, S. K. Bhatia, J. Ahn, J.-M. Jeon, J.-J. Yoon, J. Lee, Y.-H. Yang, *Polymer* **2022**, *14*, 3625.
[28] A. N. Frone, C. A. Nicolae, M. C. Eremia, V. Tofan, M. Ghiurea, I. Chiulan, E. Radu, C. M. Damian, D. M. Panaitescu, *Polymer* **2020**, *12*, 2446.
[29] T. Rakić, I. Kasagić-Vujanović, M. Jovanović, B. Jančić-Stojanović, D. Ivanović, *Anal. Lett.* **2014**, *47*, 1334.
[30] R. T. Umemura, M. I. Felisberti, *J. Appl. Polym. Sci.* **2021**, *138*, 49990.
[31] E. Blümm, A. J. Owen, *Polymer* **1995**, *36*, 4077.
[32] A. J. Owen, J. Heinzel, Ž. Škrbić, V. Divjaković, *Polymer* **1992**, *33*, 1563.
[33] M. Raimo, *ChemTexts* **2015**, *1*, 1.
[34] P. J. Barham, A. Keller, E. L. Otun, P. A. Holmes, *J. Mater. Sci.* **1984**, *19*, 2781.
[35] G. Ding, J. Liu, *Colloid Polym. Sci.* **2013**, *291*, 1547.
[36] J. D. Hoffman, J. I. Lauritzen Jr., *J. Res. Natl. Bur. Stand. A Phys. Chem.* **1961**, *65a*, 297.
[37] J. D. Hoffman, *Polymer* **1983**, *24*, 3.
[38] H. D. Keith, F. J. Padden JR, *J. Polym. Sci.* **1959**, *39*, 101.
[39] H. D. Keith, F. J. Padden Jr., *J. Polym. Sci.* **1959**, *39*, 123.
[40] H. D. Keith, F. J. Padden, *J. Appl. Phys.* **1963**, *34*, 2409.
[41] D. C. Bassett, R. H. Olley, I. A. M. Al Raheil, *Polymer* **1988**, *29*, 1539.
[42] D. Patel, D. C. Bassett, *Polymer* **2002**, *43*, 3795.
[43] D. C. Bassett, A. M. Hodge, *Proc. R. Soc. Lond. A. Math. Phys. Sci.* **1981**, *377*, 61.
[44] T. Kyu, H.-W. Chiu, A. J. Guenthner, Y. Okabe, H. Saito, T. Inoue, *Phys. Rev. Lett.* **1999**, *83*, 2749.
[45] A. J. Owen, *Polymer* **1997**, *38*, 3705.
[46] L. Zhao, X. Wang, L. Li, Z. Gan, *Polymer* **2007**, *48*, 6152.
[47] Q. Cao, X. Qiao, H. Wang, J. Liu, *Sci. China, Ser. B: Chem.* **2008**, *51*, 853.
[48] M. G. A. Vieira, M. A. da Silva, L. O. dos Santos, M. M. Beppu, *Eur. Polym. J.* **2011**, *47*, 254.
[49] H. Xiao, W. Lu, J.-T. Yeh, *J. Appl. Polym. Sci.* **2009**, *113*, 112.
[50] R. S. Kurusu, C. A. Siliki, É. David, N. R. Demarquette, C. Gauthier, J.-M. Chenal, *Ind. Crop. Prod.* **2015**, *72*, 166.
[51] M. Terada, R. H. Marchessault, *Int. J. Biol. Macromol.* **1999**, *25*, 207.
[52] A. Hussain, M. A. Altamimi, S. Alshehri, S. S. Imam, *J. Mol. Liq.* **2021**, *328*, 115432.
[53] L. Aliotta, I. Canesi, A. Lazzeri, *Polym. Test.* **2021**, *98*, 107163.
[54] J. K. Hobbs, T. J. McMaster, M. J. Miles, P. J. Barham, *Polymer* **1998**, *39*, 2437.
[55] W. Wang, E. Diao, H. Zhang, Y. Dai, H. Hou, H. Dong, *J. Appl. Polym. Sci.* **2015**, *132*, 42544.
[56] Z. Z. Fu, Y. H. Yao, S. J. Guo, K. Wang, Q. Zhang, Q. Fu, *Macromol. Rapid Commun.* **2023**, *44*, 2200296.
[57] H. D. Keith, F. J. Padden, *J. Appl. Phys.* **1964**, *35*, 1270.
[58] E. Piorkowska, Z. Kulinski, A. Galeski, R. Masirek, *Polymer* **2006**, *47*, 7178.
[59] S. Pak, S. Park, Y. S. Song, D. Lee, *Compos. Struct.* **2018**, *193*, 73.
[60] D. A. D'Amico, V. P. Cyras, L. B. Manfredi, *Thermochim. Acta* **2014**, *594*, 80.
[61] S. Duangphet, D. Szegda, K. Tarverdi, J. Song, *Key Eng. Mater.* **2017**, *751*, 242.
[62] D. Puglia, E. Fortunati, D. A. D'Amico, L. B. Manfredi, V. P. Cyras, J. M. Kenny, *Polym. Degrad. Stab.* **2014**, *99*, 127.
[63] S. Ouchiar, G. Stoclet, C. Cabaret, V. Gloaguen, *Macromolecules* **2016**, *49*, 2782.
[64] S. Akhtar, C. W. Pouton, L. J. Notarianni, *J. Control. Release* **1991**, *17*, 225.
[65] Y.-X. Weng, X.-L. Wang, Y.-Z. Wang, *Polym. Test.* **2011**, *30*, 372.
[66] X. Wen, X. Lu, Q. Peng, F. Zhu, N. Zheng, *J. Therm. Anal. Calorim.* **2012**, *109*, 959+.
[67] L. Gránásy, T. Pusztai, G. Tegze, J. A. Warren, J. F. Douglas, *Phys. Rev. E* **2005**, *72*, 72.
[68] B. Crist, J. M. Schultz, *Prog. Polym. Sci.* **2016**, *56*, 1.
[69] H. Yu, M. Zhu, Y. Zhang, Y. Chen, *Polym.-Plast. Technol. Eng.* **2004**, *43*, 1.
[70] J. Antony, in *Design of Experiments for Engineers and Scientists*, Second ed. (Ed: J. Antony), Elsevier, Oxford **2014**, p. 19. https://doi.org/10.1016/B978-0-08-099417-8.00003-1
[71] J. Antony, in *Design of Experiments for Engineers and Scientists*, Second ed. (Ed: J. Antony), Elsevier, Oxford **2014**, p. 33. https://doi.org/10.1016/B978-0-08-099417-8.00004-3
[72] R. F. Gunst, R. L. Mason, *How to construct fractional factorial experiments*, ASQC Quality Press, Milwaukee **1991**.

SUPPORTING INFORMATION

Additional supporting information can be found online in the Supporting Information section at the end of this article.

How to cite this article: K. Majerczak, J. Liggat, *J. Appl. Polym. Sci.* **2023**, *140*(40), e54469. https://doi.org/10.1002/app.54469